


## Search for polarized antiproton production

D. Grzonka<sup>1</sup>  · D. Alfs<sup>1,2</sup> · A. Asaturyan<sup>3</sup> · M. Carmignotto<sup>4</sup> · M. Diermaier<sup>5</sup> · W. Eyrich<sup>6</sup> · B. Głowacz<sup>2</sup> · F. Hauenstein<sup>7</sup> · T. Horn<sup>4</sup> · K. Kilian<sup>1</sup> · D. Lersch<sup>1</sup> · S. Malbrunot-Ettenauer<sup>8</sup> · A. Mkrtchyan<sup>3</sup> · H. Mkrtchyan<sup>3</sup> · P. Moskal<sup>2</sup> · P. Nadel-Turonski<sup>9</sup> · W. Oelert<sup>10</sup> · J. Ritman<sup>1</sup> · T. Sefzick<sup>1</sup> · V. Tadevosyan<sup>3</sup> · E. Widmann<sup>5</sup> · M. Wolke<sup>11</sup> · S. Zhamkochyan<sup>3</sup> · M. Zieliński<sup>2</sup> · A. Zink<sup>12</sup> · J. Zmeskal<sup>5</sup>

Published online: 12 March 2019  
© Springer Nature Switzerland AG 2019

### Abstract

The production of antiprotons is studied in view of possible polarization effects as basis for a polarized antiproton beam. If antiprotons are produced with some polarization, a quite simple procedure for the generation of a polarized antiproton beam could be worked out. The experiments are performed at the CERN PS test beam T11 where secondary particles with momenta around  $3.5 \text{ GeV}/c$  are selected. The polarization analysis is performed by measuring the asymmetry of the elastic  $\bar{p}p$ -scattering in the Coulomb-nuclear interference region. The detection system includes Cherenkov and tracking detectors for the particle identification and the 3d track reconstruction. Details on the detection system and the status of the analysis are given.

**Keywords** Polarized antiproton · CNI · Elastic scattering · DIRC · Drift chamber · Track reconstruction

**PACS** 24.70.+s

### 1 Introduction

The analysis of antiproton production in view of polarization effects is motivated by the request for a polarized antiproton beam. For particles like protons polarized beams are routinely prepared by separating one spin state in a magnetic field gradient acting on the magnetic moment of an atom. In case of antiprotons, antihydrogen atoms can be produced, however, the number is much too low for a reasonable polarized beam production and

---

This article is part of the Topical Collection on *Proceedings of the 13th International Conference on Low Energy Antiproton Physics (LEAP 2018) Paris, France, 12-16 March 2018*  
Edited by Paul Indelicato, Dirk van der Werf and Yves Sacquin

✉ D. Grzonka  
d.grzonka@fz-juelich.de

Extended author information available on the last page of the article.

with the eight orders of magnitude smaller nuclear magnetic moment a simple spin state separation of antiprotons in a magnetic field gradient is not possible.

Nevertheless, a polarized antiproton beam is essential for various topics. Polarization observables allow for the extraction of more detailed information of the structure of hadrons and their interaction and the disentangling of various reaction mechanisms is often only possible by a separation of different spin configurations. Possible methods for polarization are discussed since the first antiproton beams became available [1] but up to now there is no simple procedure for the preparation of a polarized antiproton beam. For most of the proposed techniques, see [2–4], the expected intensity and polarization is very low and not useful for a reasonable polarized beam. The only experiments with polarized antiprotons so far have been performed at FERMILAB by generating a polarized  $\bar{p}$ -beam via the parity violating  $\bar{\Lambda}$ -decay,  $\bar{\Lambda} \rightarrow \bar{p} + \pi^+$  resulting in  $\bar{p}$  with a helicity of -0.64. The  $\bar{\Lambda}$ 's were produced by a 800 GeV/c proton beam and a 200 GeV/c transverse polarized  $\bar{p}$ -beam was selected with a mean polarization of 0.45 and an intensity of  $10^4 \bar{p}/s$  [5]. Similar experiments are planned at the U-70 accelerator of IHEP in the SPACHARM project which is currently under development [6]. Another promising technique proposed by the PAX collaboration [7] is the spin filter method which is currently the favored solution for the preparation of a polarized  $\bar{p}$ -beam. Here an unpolarized  $\bar{p}$ -beam is circulating in a storage ring passing through an internal polarized atomic beam target and due to the spin dependent interaction one spin component is more depleted resulting in an increase of the polarization. Feasibility studies performed with protons show a clear polarization increase with storage time [8, 9]. In principle the method works also for antiprotons but it requires some instrumental effort.

A rather simple polarized beam preparation could be performed if the production process itself generates some polarization [10, 11]. In that case the separation of a certain azimuthal angular range results directly in a polarized beam. But up to now a possible polarization of produced antiprotons has never been checked experimentally. In order to investigate this possibility, measurements of the polarization of produced antiprotons have been started at a CERN/PS test beam.

## 2 Polarization measurement

The determination of the antiproton polarization will be performed by measuring the right/left asymmetry of the elastic  $\bar{p}p$ -scattering given by:  $d\sigma/(d\theta d\phi) = d\sigma/d\theta(1 + A_Y \cdot P \cdot \cos(\phi))$  for a transversely polarized beam with analyzing power  $A_Y$  and polarization  $P$ . In order to measure a polarization the analyzing power has to be well known which is the case for the Coulomb-nuclear interference (CNI) region. At high energies and small squared four momentum transfer  $t$  the theoretical description of the analyzing power simplifies [12–14] and its calculations coincides very well with experimental data taken for elastic proton-proton scattering in the CNI region [15]. At 100 GeV/c momentum the maximum  $A_Y$  in the CNI region is 4.5% at a  $t$ -value of  $t = -0.003(\text{GeV}/c)^2$ . Due to G-parity conservation the antiproton-proton scattering will result in the same value of the analyzing power but the validity of the high energy approximations is questionable for momenta of a few GeV/c. Preliminary calculations of the analyzing power at lower beam momenta have been performed by Haidenbauer [16] in a one boson exchange model with the NN potential adjusted to experimental data of  $\bar{p}p$  scattering [17] which are available down to about 5 GeV/c. The  $A_Y$  distributions at lower momenta are comparable to the high energy data with the same amplitude of about 4.5% at a bit lower  $t$ -value. In Fig. 1  $A_Y$  data for elastic  $pp$  scattering and the preliminary calculations for elastic  $\bar{p}p$  scattering are shown.

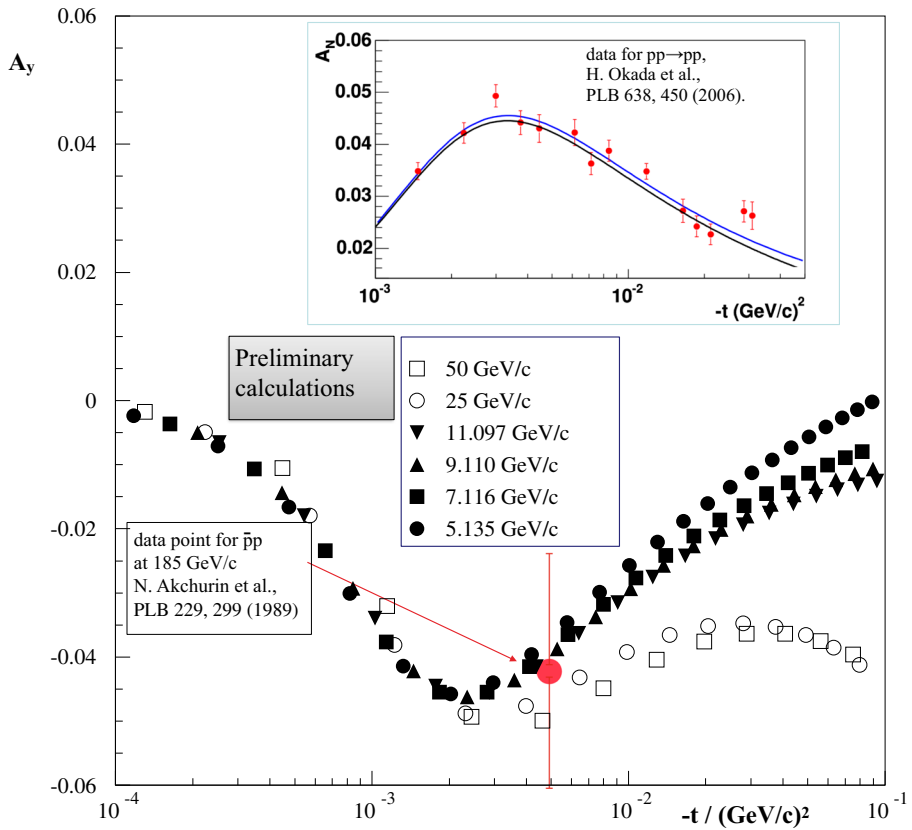


**Fig. 1** Preliminary calculations of the analyzing power  $A_y$  for elastic  $\bar{p}p$  scattering as a function of  $t$  for various beam momenta between 50 and 5  $GeV/c$  [16] with one data point measured at 185  $GeV/c$  [18](red marker). The inset in the upper part shows the available  $A_y$  data for  $pp$  scattering [15]

For the antiproton scattering only one data point is available which is consistent with the calculations but has a large error bar [18].

The experiments for measuring the antiproton polarization were performed at the CERN/PS test beam line T11. The T11 beam line delivers secondary particles produced by the 24  $GeV/c$  momentum proton beam of the CERN/PS at a production angle of about 150  $mrad$  with an acceptance of  $\pm 3 mrad$  horizontally and  $\pm 10 mrad$  vertically [19]. The beam line was adjusted for negatively charged particles of 3.5  $GeV/c$  which corresponds to the momentum used for the antiproton beam preparation at CERN/AD. The produced particles are mostly pions and only a small percentage of antiprotons is expected. From measurements at comparable conditions [20] (antiproton momentum 4  $GeV/c$ , production angle 127  $mrad$ ) the  $\bar{p}/\pi^-$ -ratio is in the order of  $10^{-3}$ . For the selection of elastic  $\bar{p}p$  scattering events the antiproton has to be identified and its track before and after the scattering process has to be measured. In the considered  $t$ -range of the CNI region the target proton will be stopped within a rather short range. Therefore, the event topology is a single track with a kink in the target volume.

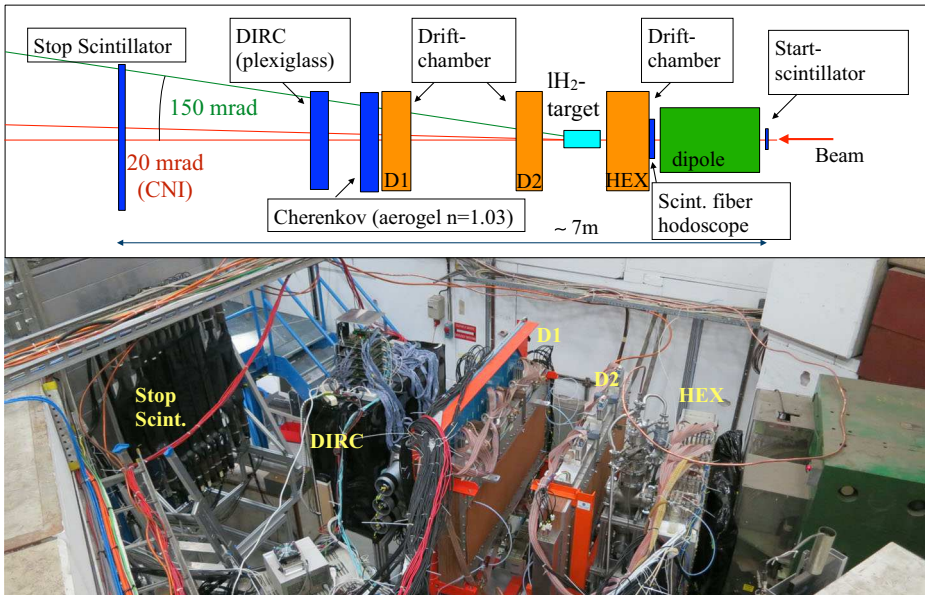


**Fig. 2** Detection setup for the antiproton polarization experiment with drift chambers for the track reconstruction and Cherenkov detectors for the particle identification. As target a 12 cm long liquid hydrogen volume is used. The start scintillator, not visible in the photo, is mounted at the entrance of the dipole at the right side

### 3 Experimental setup

In Fig. 2 a sketch and a corresponding photo of the experimental setup is shown. The particle tracks are measured with drift chambers, a single drift chamber in front of the target (HEX) and two drift chambers for the scattered particles behind the target (D1, D2), and for the particle ID Cherenkov detectors, an aerogel threshold Cherenkov counter and a plexiglas DIRC, were used. A scintillating fiber hodoscope was installed as beam monitor in front of the first drift chamber and plastic scintillators were used for the trigger signal generation. As trigger signal a coincidence between start- and stop-scintillators with a veto from the aerogel Cherenkov counter was used. The aerogel has a refractive index of  $n=1.03$  in which only pions with a threshold value of  $n=1.0008$  at  $3.5 \text{ GeV}/c$  momentum will create Cherenkov light but not the antiprotons with a threshold value of  $n=1.035$ . The spill length of the beam was about 400 ms with up to  $5 \cdot 10^5$  particles. With this Cherenkov veto signal an online pion reduction by a factor of about 30 to 40 was done resulting in trigger rates of a few 10 kHz which could be handled by the data acquisition system. In Fig. 3 left upper part the pion reduction is demonstrated for positively charged particles at lower beam momenta. At  $1 \text{ GeV}/c$  pions and protons are well separated by the time of flight between start- and stop-scintillators and the data with Cherenkov veto on (red histogram) show a strong pion reduction compared to the data with veto off (black histogram).

For the final antiproton identification the offline analysis of the DIRC signals is used. In the plexiglas radiator also antiprotons create Cherenkov light and the particle identification is done via the reconstructed Cherenkov cone angle. The photon distribution summed up for

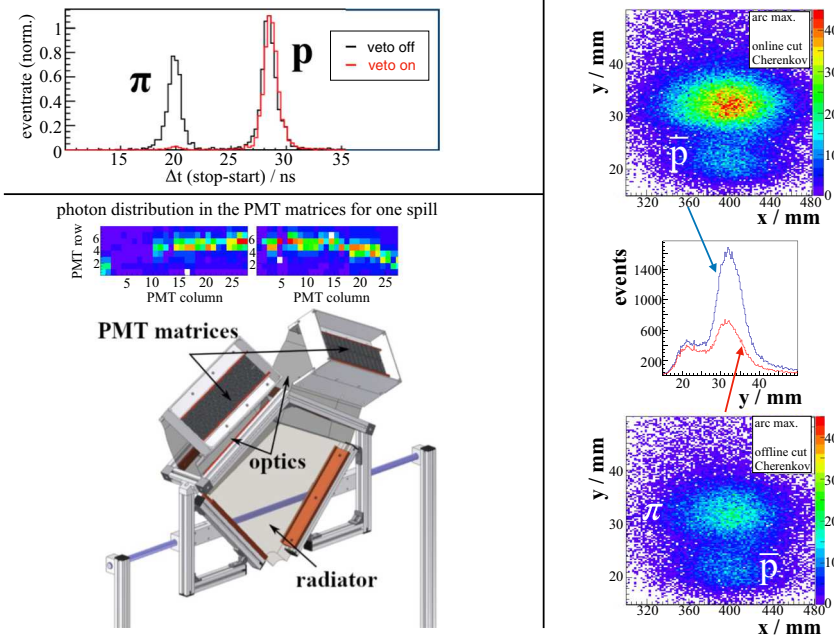


**Fig. 3** Performance of aerogel Cherenkov and DIRC. Left upper part: online pion reduction by using the aerogel Cherenkov counter signals as veto demonstrated for  $\pi^+$  / proton at  $1\text{ GeV}/c$ . Left lower part: sketch of the DIRC with a summed photon distribution for one spill. Right: Separation of  $\pi^-$  and  $\bar{p}$  by fitting the arc for individual events

a sample of events (see Fig. 3 left lower part) shows a well defined arc resulting essentially from pions. A simple parabola fit to the separate events results in a clear separation of pions and antiprotons as shown in Fig. 3 on the right side. In the upper part the arc maxima ( $y$ ) vs its horizontal position ( $x$ ) is shown for a sample with online pion reduction and in the lower part a more restrictive cut on the aerogel Cherenkov signals is performed offline which essential further reduces the pion content as seen in the projection on the  $y$ -axis. But the photon distributions for a single event are much less conclusive and depend on the track direction and hit position on the DIRC. Therefore, a simple arc fit is not sufficient but a comparison to Monte Carlo generated photon distributions has to be done for an optimum particle identification. For each event the probability of being a pion or antiproton will be calculated by a comparison with track angle and position dependent MC generated photon distributions. A rough estimate from a preliminary analysis results in a pion background of about 10% in a selected antiproton sample.

The elastic scattering events are selected by the track reconstruction in the drift chambers. Two types of drift chambers are used, D1 and D2 with rectangular drift cells with a width of  $\pm 2\text{ cm}$  and HEX with a hexagonal drift cell structure and a sense wire distance of  $1.8\text{ cm}$ . Vertical and inclined wires,  $\pm 31\text{ deg}$  for D1, D2 and  $\pm 11\text{ deg}$  for HEX, allow a 3d reconstruction of particle tracks before and after passing through the target. The calibration of the drift chamber results in position resolutions of  $150 - 300\ \mu\text{m}$  from which a track

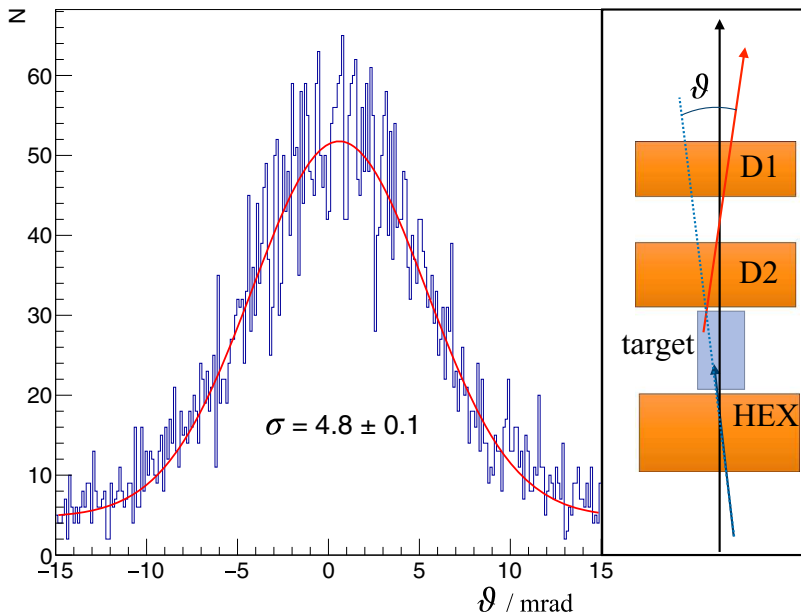


**Fig. 4** Estimation of the resolution for the scattering angle reconstruction. The procedure is sketched on the right side. Events are selected by a reasonable single track fit with all drift chamber signals (black line) and then separate track fits for HEX (blue line) and D1/D2 (red line) are performed

resolution of below 1 *mrad* results. The expected precision for the measurement of the scattering angle is a few *mrad* by including the straggling in the material on the path of the antiprotons. From the data an actual resolution of about 5 *mrad* (FWHM) is estimated (Fig. 4) which will be further improved by a fine tuning of the calibration and the relative chamber positioning. For details on the analysis see [21]. The resolution is sufficient to separate the scattering events in the relevant angular range of 10 - 20 *mrad*.

In order to increase the statistics an additional measurement with an improved detection setup is performed in 2018. Fig. 5 shows a sketch of the new setup with essentially similar components, scintillators, tracking and Cherenkov detectors. A trigger signal will be generated by a small 2 cm x 2 cm plastic scintillator with a veto from aerogel Cherenkov counters directly behind the trigger scintillator. The Cherenkov counter includes a 10 cm long aerogel tube with a diameter of 3 cm and the Cherenkov photons are reflected at a mirror foil into photomultipliers on both sides. For the primary track a scintillating fiber hodoscope will be used with 0.25 mm scintillating fibers readout with SiPM arrays. It includes two modules with double layers of scintillating fibers in x and y-direction separated by 40 cm. The tracks of the scattered particles will be measured with straw tubes, two modules with 3 double layers in vertical direction and rotated by  $\pm 60$  deg. Both tracking detector systems will give track resolution of below 1 *mrad*. The target and the DIRC will be the same as used in the previous measurement. All detector components are mounted on one common frame which simplifies the geometrical adjustment.

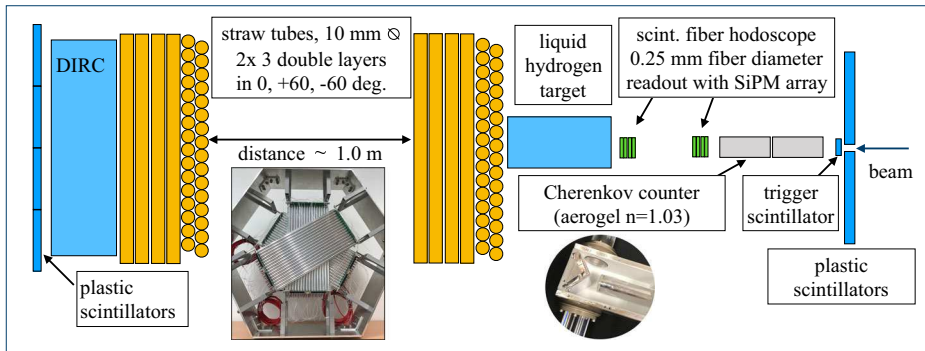


**Fig. 5** Sketch of the detection system for the follow-up experiment. In the lower part photos of a straw tube module showing the orientation of the straw tube planes and an open Cherenkov counter module with the aerogel tube and the mirror foil reflecting the photons to the photomultipliers on both sides

## 4 Summary

In order to measure the polarization of antiprotons produced in  $pA$  interactions in view of a polarized antiproton beam data have been taken at the CERN PS test beam. Statistics will be increased by a follow-up experiment with an improved detection system. Both systems include tracking and Cherenkov detectors which allow to identify the particle ID and to reconstruct the scattering angle to determine the polarization. The data are presently under analysis. The track reconstructions with the existing data achieve the expected resolution and with the photon distributions in the DIRC the antiprotons can be well separated from the pion background. Currently a fine tuning of the drift chamber calibration and positioning for an improved resolution and the particle identification from the photon distributions in the DIRC supported by simulation studies are performed. Furthermore, the detector components for the follow-up experiment are prepared.

**Acknowledgements** This work was supported by Marie Skłodowska-Curie Innovative Training Network Fellowship of the European Commission's Horizon 2020 Programme (No. 721559 AVA), the Polish Ministry of Science and Higher Education and DAAD from resources of Bundesministerium für Bildung und Forschung (BMBF), by Marian Smoluchowski Krakow Research Consortium "Matter-Energy-Future" (KNOW) and the Polish Ministry of Science and Higher Education through grant number 7150/E-338/M/2018.


## References

1. Krisch, A.D.: Summary of workshop on polarized anti-proton sources. AIP Conf. Proc. **145**, 215–220 (1986)
2. Steffens, E.: Polarized antiprotons - the quest for a missing tool. AIP Conf. Proc. **1149**, 80–89 (2009)
3. Meyer, H.O.: Workshop summary on polarized antiproton beams. AIP Conf. Proc. **1008**, 124–131 (2008)
4. Schoch, B.: A method to polarise antiprotons in storage rings and create polarized antineutrons. Eur. Phys. J. A **43**, 5–9 (2010)
5. Bravar, A., et al.: Single-spin asymmetries in inclusive charged pion production by transversely polarized antiprotons. Phys. Rev. Lett. **77**, 2626–2629 (1996)
6. Abramov, V.V., et al.: Production asymmetry measurement of high  $x_T$  hadrons in pp collisions at 40 GeV. Nucl. Instrum. Meth. A **901**, 62–68 (2018)

7. Lenisa, P., Rathmann, F., for the PAX collaboration: Antiproton-proton scattering experiments with polarization arXiv:[hep-ex/0505054v1](https://arxiv.org/abs/hep-ex/0505054v1) (2005)
8. Rathmann, F., et al.: New method to polarize protons in a storage ring and implications to polarize antiprotons. *Phys. Rev. Lett.* **71**, 1379–1382 (1993)
9. Augustyniak, W., et al.: Polarization of a stored beam by spin-filtering. *Phys. Lett. B* **718**, 64–69 (2012)
10. Kilian, K., et al.: Ways to make polarized antiproton beams. *Int. J. Mod. Phys. A* **26**, 757 (2011)
11. Grzonka, D., et al.: Search for polarization effects in the antiproton production process. *Acta. Phys. Polon. B* **46**, 191 (2015)
12. Kopeliovich, B.Z., Lapidus, L.I.: On the necessity of polarization experiments on colliding  $p - p$  and  $\bar{p} - p$  beams. *Sov. J. Nucl. Phys.* **19**, 114 (1974)
13. Akchurin, N., et al.: Analyzing power measurement of pp elastic scattering in the coulomb-nuclear interference region with the 200-GeV/c polarized-proton beam at Fermilab. *Phys. Rev. D* **48**, 3026 (1993)
14. Buttimore, N.H., et al.: The spin dependence of high-energy proton scattering. *Phys. Rev. D* **59**, 114010–114057 (1999)
15. Okada, H., et al.: Measurement of the analyzing power in pp elastic scattering in the peak CNI region at RHIC. *Phys. Lett. B* **638**, 450–454 (2006)
16. Haidenbauer, J.: Calculation of  $a_Y$  in  $\bar{p}p$  scattering private communication (2014)
17. Haidenbauer, J., Krein, G.: Production of charmed pseudoscalar mesons in antiproton-proton annihilation. *Phys. Rev. D* **114003**, 89 (2014)
18. Akchurin, N., et al.: Analyzing-power measurements of coulomb-nuclear interference with the polarized-proton and -antiproton beams at 185 GeV/c. *Phys. Lett. B* **229**, 299–303 (1989)
19. [http://sba.web.cern.ch/sba/Documentations/Eastdocs/docs/T11\\_Guide.pdf](http://sba.web.cern.ch/sba/Documentations/Eastdocs/docs/T11_Guide.pdf)
20. Eichten, T., et al.: Particle production in proton interactions in nuclei at 25 GeV/c. *Nucl. Phys. B* **44**, 333–343 (1972)
21. Alfs, D., et al.: Drift chamber calibration and track reconstruction in the P349 antiproton polarization experiment. *Acta. Phys. Polon. B* **48**, 1983 (2017)

**Publisher's note** Springer Nature remains neutral with regard to jurisdictional claims in published maps and institutional affiliations.

## Affiliations

D. Grzonka<sup>1</sup>  · D. Alfs<sup>1,2</sup> · A. Asaturyan<sup>3</sup> · M. Carmignotto<sup>4</sup> · M. Diermaier<sup>5</sup> · W. Eyrich<sup>6</sup> · B. Głowacz<sup>2</sup> · F. Hauenstein<sup>7</sup> · T. Horn<sup>4</sup> · K. Kilian<sup>1</sup> · D. Lersch<sup>1</sup> · S. Malbrunot-Ettenauer<sup>8</sup> · A. Mkrtchyan<sup>3</sup> · H. Mkrtchyan<sup>3</sup> · P. Moskal<sup>2</sup> · P. Nadel-Turonski<sup>9</sup> · W. Oelert<sup>10</sup> · J. Ritman<sup>1</sup> · T. Sefzick<sup>1</sup> · V. Tadevosyan<sup>3</sup> · E. Widmann<sup>5</sup> · M. Wolke<sup>11</sup> · S. Zhamkochyan<sup>3</sup> · M. Zieliński<sup>2</sup> · A. Zink<sup>12</sup> · J. Zmeskal<sup>5</sup>

<sup>1</sup> Institut für Kernphysik, Forschungszentrum Jülich, Jülich, Germany

<sup>2</sup> M. Smoluchowski Institute of Physics, Jagiellonian University, Krakow, Poland

<sup>3</sup> A.I. Alikhanyan Science Laboratory, Yerevan, Armenia

<sup>4</sup> Physics Department, The Catholic University of America, Washington, DC, USA

<sup>5</sup> Stefan-Meyer-Institut für subatomare Physik, Wien, Austria

<sup>6</sup> Universität Erlangen, Erlangen, Germany

<sup>7</sup> Old Dominion University, Norfolk, VA, USA

<sup>8</sup> Physics Department, CERN, Geneva, Switzerland

<sup>9</sup> Thomas Jefferson National Accelerator Facility, Newport News, VA, USA

<sup>10</sup> Johannes Gutenberg-Universität Mainz, Mainz, Germany

<sup>11</sup> Department of Physics and Astronomy, Uppsala University, Uppsala, Sweden

<sup>12</sup> Erlangen Centre for Astroparticle Physics (ECAP), Erlangen, Germany